AIAA JOURNAL
Vol. 40, No. 11, November 2002

Structure and Extinction of Heptane/Air Partially Premixed Flames

Hongshe Xue* and Suresh K. Aggarwal†
University of Illinois at Chicago, Chicago, Illinois 60607

A numerical investigation of the structure and extinction of n-heptane/air partially premixed flames in a counterflow configuration is reported. The flame is computed using a detailed reaction mechanism consisting of 275 elementary reactions and 41 species. The mechanism is validated by comparing its predictions with measurements for both the premixed and nonpremixed flames. The partially premixed flame structure is characterized by two-stage burning or two spatially distinct, but synergistically coupled, reaction zones, namely, a rich premixed zone on the fuel side and a nonpremixed zone on the air side. Two major pathways characterize the n-heptane/air chemistry in these two reaction zones. The fuel is completely consumed in the premixed reaction zone, with ethylene and acetylene being the major intermediate species. Interactions between the two zones involve the transport of heat from the nonpremixed to the premixed reaction zone and the transport of CO, H_2, and C_2H_2 from the premixed to the nonpremixed reaction zone. The flame response to variations in equivalence ratio and strain rate is characterized. Increasing the equivalence ratio and/or strain rate to a critical value leads to merging of the two reaction zones. Further increase in equivalence ratio leads to a nonpremixed flame, whereas that in strain rate leads to flame extinction. The partially premixed combustion regime is obtained by computing the critical strain rate for merging as a function of the equivalence ratio. The flame structure is characterized in terms of a modified mixture fraction (conserved scalar), and laminar flamelet profiles are provided. Stretch-induced extinction is also investigated. Results indicate that as the level of partial premixing is increased, the flame extinction occurs at increasingly higher strain rates, implying that partially premixed flames are less prone to extinction compared to nonpremixed flames.

Introduction

PARTIALLY premixed flames are formed by mixing air (in less than stoichiometric amounts) into the fuel stream before the reaction zone, where additional air is available for complete combustion. Using partial premixing, one can exploit the advantages of both nonpremixed and premixed flames regarding safety, lower pollutant emission levels, and flame stability. The partially premixed flames are relevant to turbulent nonpremixed combustion, which can contain regions where local extinction occurs, followed by partial premixing and reignition. Partially premixed combustion plays a fundamental role in the stabilization of lifted nonpremixed flames in which propagating premixed reaction zones anchor a nonpremixed reaction zone. Spray and droplet-group flames also contain regions of partially premixed combustion.

Because of their fundamental and practical relevance, partially premixed flames have been studied extensively in recent years. Most of these studies, however, have focused on methane–air flames,[1–4] motivated by the availability of extensive experimental data and detailed chemistry models. Except for a recent experimental study by Li and Williams,[5] the detailed structure of partially premixed flames burning higher hydrocarbon fuels, especially liquid fuels, has not been investigated. Such flames are important in many propulsion and energy-conversion applications. For instance, the combustion process in both the spark-ignition[6] and diesel[7] engines is dominated by partially premixed or two-stage combustion.

In the present study, we investigate the structure of heptane–air partially premixed flames in a counterflow configuration. To avoid complications arising due to interactions between the dispersed (droplets) and continuous phases, the fuel is considered in the prevaporized form. This allows us to focus on the detailed flame structure and the thermochemical and fluid dynamical interactions between the reaction zones. The fuel used is n-heptane, which, perhaps, is the most representative liquid fuel. It has been the fuel of choice in numerous experimental, theoretical, and computational studies dealing with spray ignition and droplet ignition,[8,9] chemical kinetics,[10,11] premixed flames,[12] droplet combustion,[13,14] soot kinetics,[15] and spray flames.[16] Although these studies have examined a variety of combustion phenomena, they have not focused on partially premixed combustion. The present work is motivated by this consideration.

A partially premixed flame is characterized by the presence of spatially distinct but synergistically coupled multiple reaction zones. There may be significant differences between higher-hydrocarbon flames and methane flames with respect to the dominant reaction pathways and, consequently, the interactions between the reaction zones. This has important implications for flame stability, pollutant formation, and other related phenomena. Consequently, another objective of this investigation is to characterize interactions between the reaction zones, and the dominant pathways associated with each zone, for heptane/air partially premixed flames. This will also enable us to understand the fundamental differences between partially premixed flames burning higher hydrocarbons and those burning methane.

Another motivation for the present work is provided by recent observations of diesel engine combustion reported by Flynn et al.[7] and Dec.[17] Based on the laser-based visualization of processes of fuel vaporization, ignition, and combustion in diesel engines, they proposed that the energy release from fuel in a diesel engine essentially occurs through a partially premixed flame. In addition, processes of soot and NOx formation were shown to be strongly dependent on the chemical and fluid dynamic interactions between the rich premixed and the nonpremixed reaction zones. Consequently, it is of fundamental interest to investigate the detailed chemical structure of heptane/air partially premixed flames from considerations of soot and NOx emissions.

We first compute the structure of a counterflow heptane/air partially premixed flame using the detailed chemistry model of Held et al.[18] The flow consists of two opposing jets, one containing a rich

Received 23 August 2001; revision received 10 June 2002; accepted for publication 25 June 2002.

*Graduate Assistant, Department of Mechanical and Industrial Engineering, 842 West Taylor Street.
†Professor, Department of Mechanical and Industrial Engineering, 842 West Taylor Street; ska@uic.edu. Associate Fellow AIAA.

n-heptane/air mixture and the other containing air. In this configuration, a partially premixed flame is established that contains two reaction zones, namely, a rich premixed zone on the fuel side and a nonpremixed zone on the air side. The counterflow configuration is employed so that our investigation can focus on 1) the dominant pathways that characterize the chemical structure of the flame, 2) interactions between the two reaction zones, 3) the partially premixed flamelet response to variations in equivalence ration and strain rate, and 4) state relationships in terms of a modified conserved scalar. We also examine processes involved in the merging of the reaction zones and the stretch-induced extinction of partially premixed flames.

It is noteworthy that heptane/air chemistry has been extensively investigated, and several detailed,[10,11,19] skeletal,[20] and reduced[19,21] mechanisms have been reported. The present study employs the Held et al. mechanism because its predictions for various zero- and one-dimensional premixed,[18] as well as for nonpremixed flames involving single droplets,[14] compare well with experimental data. Also note that several recent investigations have employed detailed chemistry models to compute the structure of nonpremixed heptane/air flames in sprays[22,23] and counterflow configurations.[24,25]

Physical–Numerical Model

The physical model considers a partially premixed flame in a counterflow configuration. The flame is established by igniting the fuel/air mixture formed by two opposing jets, one containing a rich n-heptane/air mixture and the other containing air. In this configuration, shown schematically in Fig. 1, the flame is observed to contain two spatially separated reaction zones over a wide range of equivalence ratio ϕ and aerodynamic strain rates a_s. The flame structure can be controlled by independently varying ϕ and a_s.

Simulations were performed using the OPPDIF[26] and Chemkin packages.[27] The grid independence was examined by changing the values of gradient (GRAD) and curvature (CURV). These two parameters provide the convergence criteria and also control the grid distribution and the total number of grid points. Computations were performed by using values of 0.8, 0.6, 0.3, 0.2, and 0.1 for these parameters. The results were found to be essentially identical for the last two values.

Knowledge of the flame behavior under the influence of straining is helpful for understanding turbulent flames that can be conceptually regarded as an ensemble of stretched laminar flamelets. A commonly accepted measure of an effective strain rate is the maximum axial velocity gradient right upstream of the flame on the air side.[28] This characteristic strain rate of the inner flow may be approximated from the outer flow (jet exit conditions) using the formula,[29]

$$a_s = \frac{2|v_0|}{L}\left(1 + \frac{|v_f|\sqrt{\rho_f}}{|v_o|\sqrt{\rho_o}}\right)$$

where L is the separation distance between the two jets, v_o the oxidizer jet exit velocity, v_f the fuel jet exit velocity, and ρ_f and ρ_o are the mixture densities in the fuel and oxidizer streams, respectively. In the present study, the preceding equation is used to calculate the strain rate. The plug flow boundary conditions are employed.

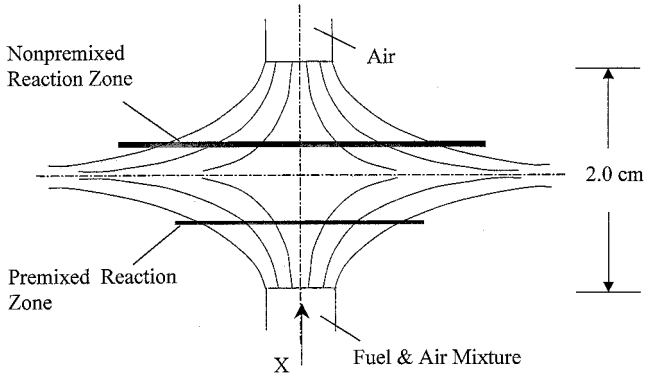

Fig. 1 Schematic of a counterflow partially premixed flame.

The exit velocities of the fuel and oxidizer streams are obtained by matching the momenta of the two streams. The strain rate is then varied by varying the velocity of the oxidizer stream. These velocities were, respectively, 16.7, 22, 30.6, 35, 61.5, and 87.5 cm/s, corresponding to the strain rates 33.4, 44, 61.2, 70, 123, and 175 s^{-1} considered in the present study. The fuel side equivalence ratio is varied as 2.0, 2.7, 3.0, 3.3, and 5.0 to study the effect of equivalence ratio on flame structure. The temperatures of the fuel and oxidizer streams are assumed to be 390 and 300 K, respectively.

The radiative heat loss is not considered in the present study. The effect of radiative heat loss is known to be important for low strain rate flames. However, the strain rates considered in the present study were not close to the limit at which the radiative heat loss becomes important.

The detailed description of the mathematical model for counterflow flames can be found elsewhere[26,30,31] and is not presented here. The n-heptane/air chemistry is modeled by using the Held et al. mechanism.[18] It involves 41 species and 275 elementary reactions.

Results and Discussion

Validation

A detailed validation of the reaction mechanism employed in this study has been provided by Held et al.[18] The computed results have been shown to compare well with experimental data for various configurations that include flow reactor, shock tube, stirred reactor, and freely propagating laminar flames. Here we provide three additional validations. For the first, the Premix[31] and Chemkin[27] packages are employed to compute the freely propagating premixed flame speed S_L of prevaporized n-heptane/air mixture as a function of the equivalence ratio ϕ. Figure 2 presents the comparison of our predictions with experimental data reported by Davis and Law.[12] The predictions show excellent agreement with the measurements. Another validation involved the comparison of our predictions with measurements of Chelliah et al.[24] for a n-heptane/air diffusion flame. The measured and computed temperature profiles indicated excellent agreement. Additional details are provided elsewhere.[32]

For a more comprehensive validation of the reaction mechanism, we computed the detailed structure of an n-heptane diffusion flame using this mechanism, and compared the predictions with the measurements of Seiser et al.[25] The velocity and temperature of the oxidizer (air) stream were 37.5 cm/s and 298 K, respectively, and those of the fuel stream were 34.2 cm/s and 338 K. The fuel stream was a mixture of n-heptane vapor and nitrogen with $X_{\text{fuel}} = 0.15$. The temperature profiles were measured using a thermocouple, whereas the species profiles were obtained using a gas chromatograph. As stated in Ref. 25, errors in composition measurements were estimated to be less than $\pm 10\%$ and those in temperature measurements less than ± 100 K. Figure 3 presents a detailed comparison of the measured and predicted flame structures in terms of the temperature, as well as the major and minor species mole fraction profiles. Both the temperature and major species profiles show good agreement

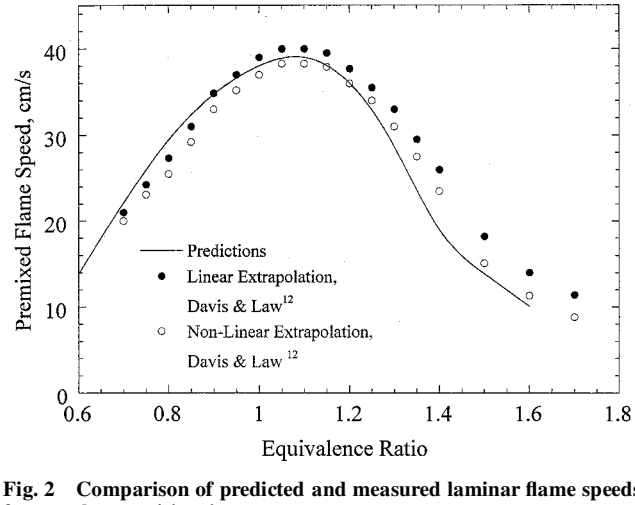

Fig. 2 Comparison of predicted and measured laminar flame speeds for an n-heptane/air mixture.

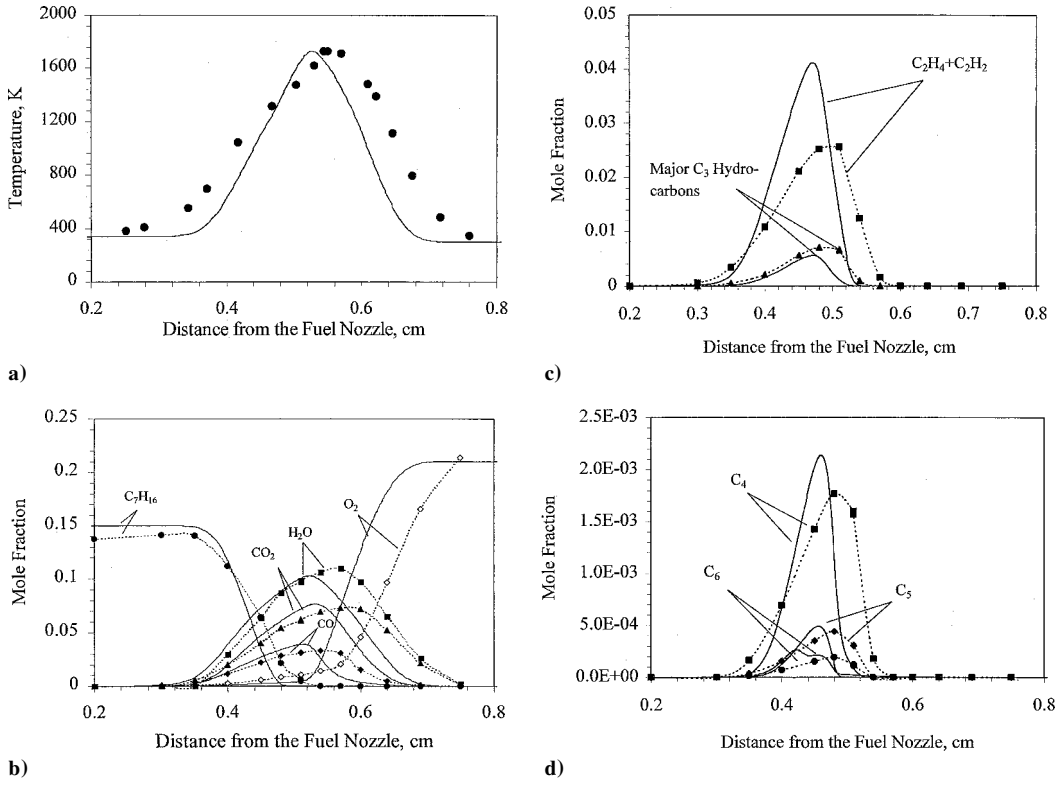

Fig. 3 Comparison between predictions and measurements of Seiser et al.[25] for a counterflow nonpremixed n-heptane/air flame, shown in terms of a) temperature profiles, b) major species mole fraction profiles, c) C_2 and C_3 species mole fraction profiles, and d) C_4, C_5, and C_6 species mole fraction profiles.

between the predictions and measurements, except that predictions locate the flame more toward the fuel side compared to measurements. As discussed by Seiser et al.,[25] this is mainly attributed to the absence of buoyancy in the numerical model. The comparison in terms of many intermediate species mole fractions is presented in Figs. 3c and 3d and provides additional validation for the n-heptane mechanism used in the present study.

Partially Premixed Flame Structure

The OPPDIF package[26] is used to compute the structure of a partially premixed heptane/air flame established at an equivalence ratio of $\phi = 2$ and a strain rate of $a_s = 33.4\ s^{-1}$. Figure 4 presents the predicted flame structure in terms of the temperature and major species mole fraction profiles. The species include the major reactant ($n\text{-}C_7H_{16}$ and O_2), intermediate (CO, H_2, C_2H_4, and C_2H_2), and product (CO_2 and H_2O) species. The flame contains two reaction zones, a rich premixed (RP) reaction zone on the fuel side and a nonpremixed (NP) reaction zone on the air side. The two reaction zones are indicated by two dark lines in Fig. 4. The location of the premixed reaction zone is determined by the maximal temperature gradient in that zone, whereas that of the NP zone is determined by the peak temperature.

The fuel is completely consumed in the premixed zone to produce CO, H_2, and C_2H_2. These three species, which represent the "intermediate fuels," are transported to the NP zone, where they are oxidized to produce CO_2 and H_2O. Consequently, the NP reaction zone chemistry is characterized by the oxidation of CO, H_2, and C_2H_2 species, whereas the chemistry for the conversion of fuel to CO is dominant in the premixed zone. The conversion of C_2H_2 to CO occurs in both the reaction zones.

We have identified the dominant pathways associated with each reaction zone by using the rate of production analysis. For each individual species, all of the reactions involving that species are compared, and the dominant production and consumption reactions are identified. Although the details are provided elsewhere,[32] the important results are summarized in Figs. 5 and 6. Two major pathways are identified. In the first, n-heptane reduces to methyl, ethyl, and ethylene through direct decomposition, atomic hydrogen abstraction,

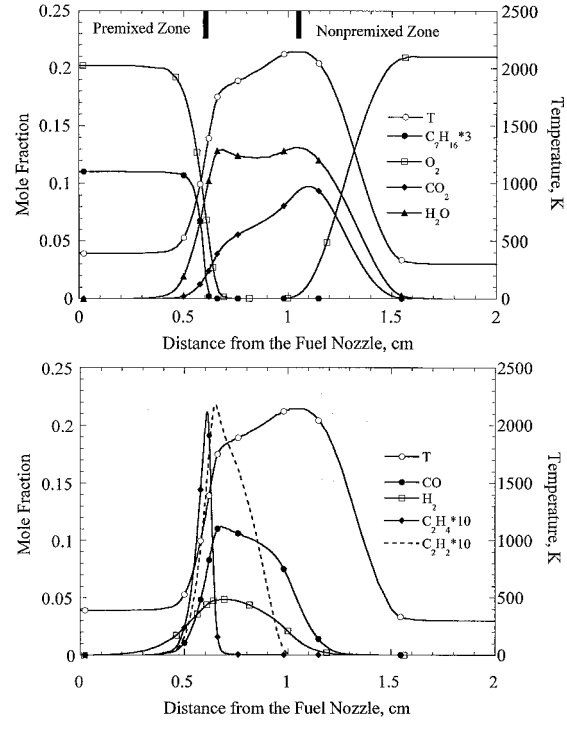

Fig. 4 Predicted temperature and major species mole fraction profiles for an n-heptane/air partially premixed flame at $\phi = 2.0$ and $a_s = 33.4\ s^{-1}$; the location of the two reaction zones is indicated by two dark lines.

and β-scission reactions. These species are subsequently converted to CO. The recombination of methyl radical produces ethane and ethyl and reinforces the C_2 chain.

The second path for fuel consumption occurs through the production of C_3–C_6 olefins (cf. Fig. 5b), which subsequently form C_3H_5. C_3H_5 combines with methyl, producing C_4H_6, which is converted to C_2H_3HCO, C_2H_4, and C_2H_3, which subsequently form CO and C_2H_2. The further oxidation of C_2H_2 follows the same path

as indicated in Fig. 5a. Additional details are provided in Fig. 6. In Fig. 6, the − and + signs, respectively, indicate the consumption and production of a particular species, and the corresponding numbers denote the mole percentage of the species consumed or produced. The mole fraction profiles for the C_2–C_6 species (not shown) indicated that all of these species are present only in the premixed region except for C_2H_2, which extends over to the NP zone (cf. Fig. 4b). In the premixed zone, the mole fractions of C_2H_4 and C_2H_2 are significantly higher, as much as 10 times, than those of other intermediate species such as C_3–C_6 olefins (cf. Fig. 4b). As illustrated in Fig. 5, ethylene is mainly produced through the direct decomposition of fuel and the reduction of as C_3–C_6 olefins in the premixed zone. As indicated in Fig. 4b, it is also consumed in the premixed zone to produce C_2H_2. Acetylene formed in the premixed zone is transported to the NP zone, which constitutes an important interaction between the two reaction zones. This is clearly illustrated in Fig. 7, which shows the net reaction rate profile of acetylene. The consumption rates of acetylene in the two reaction zones are nearly equal.

In summary, the oxidation of n-heptane under partial premixing follows two paths. The first path mainly consists of C_2 chemistry, including the conversion of ethane to acetylene, and the oxidation of acetylene to CO. The first part of this pathway occurs in the premixed zone with C_2H_2 being the product, which is consumed in both the premixed and NP reaction zones. The second path starts with the decomposition of C_3–C_6 species to C_3H_5, followed by the conversion of C_3H_5 to C_4H_6, which is finally converted to vinyl and acetylene as well as C_2H_3HCO. The second path mainly occurs in the RP reaction zone.

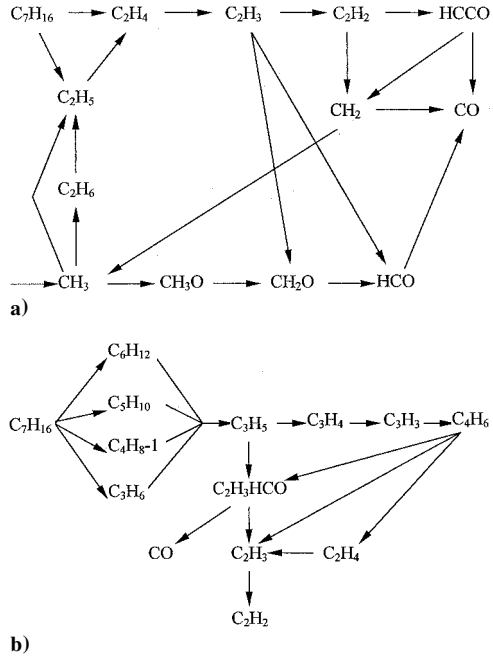

Fig. 5 Dominant pathways for n-heptane oxidation for an n-heptane/air partially premixed flame at $\phi = 2.0$ and $a_s = 33.4\ s^{-1}$.

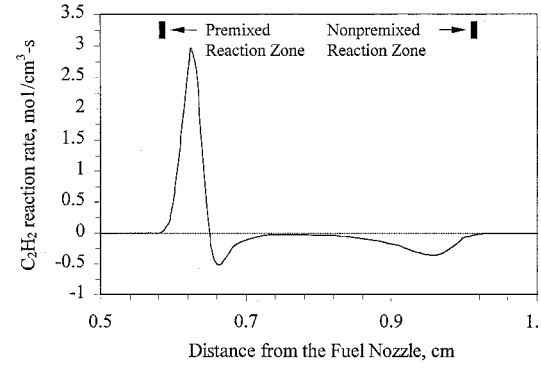

Fig. 7 Acetylene net reaction rate profile for the conditions of Fig. 6.

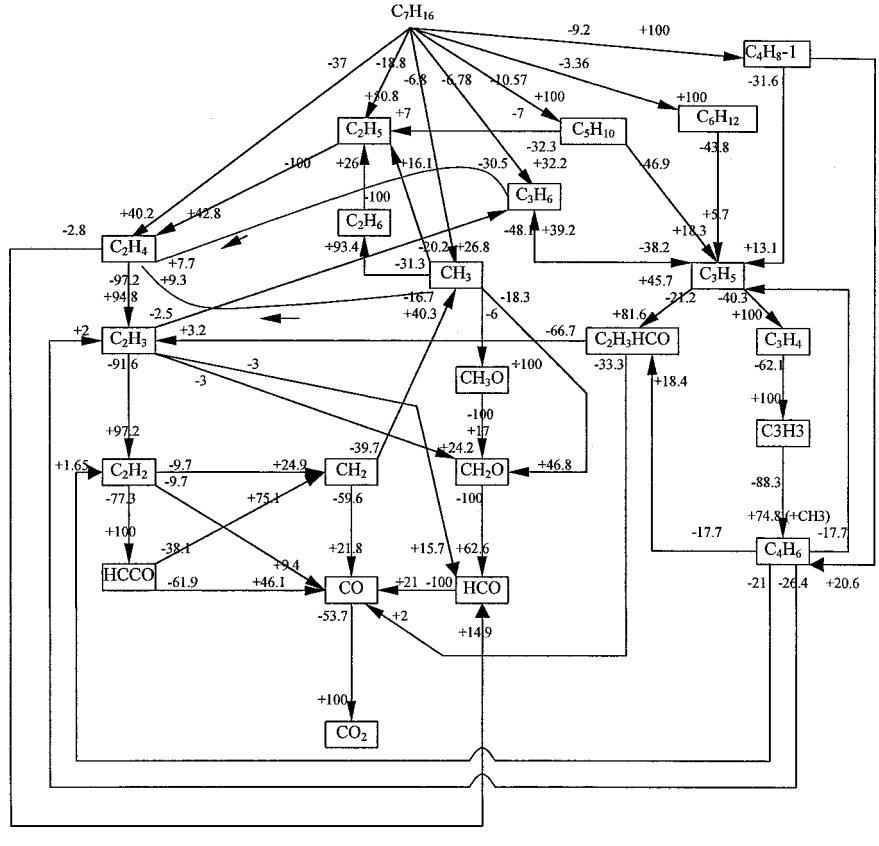

Fig. 6 Detailed pathways for n-heptane oxidation for an n-heptane/air partially premixed flame at $\phi = 2.0$ and $a_s = 33.4\ s^{-1}$; the − and + signs, respectively, indicate the consumption and production of a particular species.

Difference Between Methane and n-Heptane Partially Premixed Flame Structures

The global structures of n-heptane and methane partially premixed flames are generally similar in that they both contain two reaction zones, namely an RP zone on the fuel side and an NP zone on the oxidizer side. There are also fundamental similarities between the structures of these flames. For both cases, the fuel is oxidized in the RP zone with CO and H_2 being the major products, which are then transported to the NP zone. The chemistry in the NP zone is characterized by the oxidation of these intermediate fuels. The two flames also exhibit important structural differences, however. Because n-heptane is a higher alkane than methane, the fuel oxidation chemistry in the RP reaction zone is significantly more complex for the former. The dominant pathways associated with heptane oxidation and methane oxidation in the RP zone are discussed in Refs. 32 and 33, respectively. An important consequence of different pathways is that in addition to CO and H_2, C_2H_2 represents another intermediate fuel for the n-heptane flame.

Another difference between the methane and n-heptane partially premixed flames pertains to the transport of H and OH radicals between the two reaction zones. Our previous investigation of methane/air partially premixed flames[1] have shown that the transport H and OH radicals from the NP to premixed reaction zone represents an essential aspect of interaction between the two zones. To examine this aspect for heptane/air flames, we present in Fig. 8 the temperature profile and the total mass flux profiles of H and OH radicals. The total mass flux is calculated by adding the convective and diffusive mass fluxes, that is, $\rho Y_i (V + V_{i,\,\mathrm{dif}})$, where ρ is the mixture density, V the mixture velocity, and Y_i and $V_{i,\mathrm{dif}}$ the mass fraction and diffusion velocity, respectively, of species i. A positive value of the mass flux indicates that the direction of mass flux is toward the oxidizer boundary and vice versa. Then, from the species conservation equation, it can be easily inferred that the positive-sloped portion of the mass flux profile implies that species is produced, whereas the negative-sloped portion indicates consumption. The mass flux profiles of H and OH for $\phi = 2.0$ are presented in Fig. 8a. The two reaction zones can be easily identified from the mass flux profiles. These profiles also indicate that the transport of H and OH radials from the NP to the premixed zone is negligible. The premixed zone can, therefore, be regarded as "self-supported" in the context of species transport. This observation is found to be valid as ϕ is varied from 1.5 to 3.3. For $\phi > 3.3$, the two reaction zones are observed to merge into a NP flame.

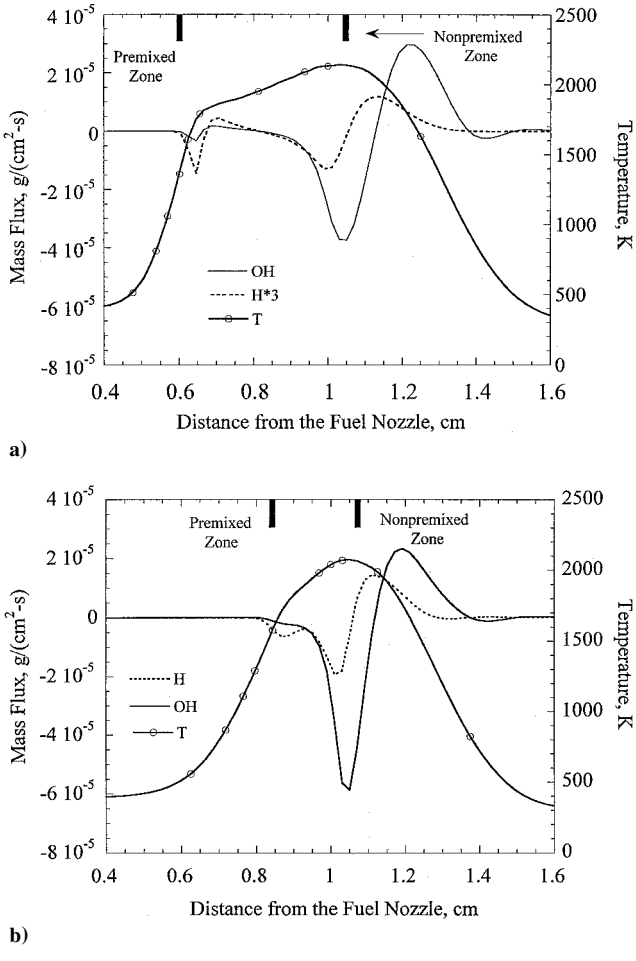

Fig. 8 Temperature and H and OH mass flux profiles for partially premixed flames at a) $\phi = 2.0$ and b) $\phi = 3.34$; the strain rate is 33.4 s^{-1}.

The merging process is evident in Fig. 8b, which shows the temperature and H and OH mass flux profiles for $\phi = 3.34$. In contrast to those for $\phi < 3.34$, the mass flux profiles at $\phi = 3.34$ increase to a nonzero value before they decrease again in the NP zone. This indicates that H and OH radicals produced in the NP zone begin to enter the premixed zone. Thus, the premixed zone is not self-supported any more and is about to merge with the NP zone. Thus, $\phi = 3.34$ can be considered as the critical equivalence ratio for merging at $a_s = 33.4\ s^{-1}$. Consequently, for heptane/air partially premixed flames, interactions between the two reaction zones are characterized by the transport of intermediate species, namely, CO, H_2, and C_2H_2, from the premixed to the NP zone and the transport of heat from the NP to the premixed zone.

Effect of Equivalence Ratio

It has been recognized that the two reaction zones of a partially premixed flame merge as ϕ and/or a_s are increased. However, differences between the effects of ϕ and a_s on the merging process have not been clearly identified in previous studies. In this section, the response of heptane/air partially premixed flames to variations in ϕ and a_s is characterized.

The flame response to the equivalence ratio variation was investigated by examining the mass flux and reaction rate profiles of H and OH radicals for flames established at different ϕ but at a fixed strain rate of $a_s = 33.4\ s^{-1}$. It was observed that as ϕ is increased, the spatial separation between the two reaction zones is reduced, and, thereby, their interaction is enhanced. In addition, premixed zone becomes increasingly weaker and more dependent on the heat transport from the NP zone. The two reaction zones were found to merge at $\phi \approx 3.34$. Unlike methane, it seems that the equivalence ratio for merging of n-heptane partially premixed flames is close to the rich flammability limit. This, however, remains open to debate because, according to the laminar flame speed data reported by Davis and Law,[12] the flammability limits of an n-heptane/air mixture appear to be $0.7 \leq \phi \leq 1.7$.

The reaction rate profiles of H and OH at different ϕ indicated that OH radical plays a key role in the merging process. As ϕ increases, or the level of partial premixing decreases, it causes a deficiency of OH radical (due to a reduction in O_2 concentration). This leads to a reduction in the CO oxidation rate in the premixed zone. In summary, as ϕ is increased, the merging of the reaction zones results from the weakening of the premixed zone, caused primarily by the deficiency of OH radical in this zone.

Effect of Strain Rate

Because of its direct relevance to turbulent flames, the response of NP and premixed methane/air flames to the strain rate variation has been extensively studied. Law et al.[34] observed that methane/air premixed flames are relatively insensitive to variations in the strain rate, as long as it is far from the critical extinction value. In contrast, the methane/air NP flames were recognized as being sensitive to strain rate. Increasing the strain rate increases the fuel and oxidizer concentration gradients in the mixing layer, thereby decreasing the local diffusion time in the vicinity of the flame. Consequently, the flame is subjected to increasingly larger nonequilibrium effects, which eventually results in stretch-induced extinction. To the best of our knowledge, the response of heptane/air partially premixed flames to strain rate variations has not been previously investigated. In addition, the partially premixed flames can be used to examine the relative effects of strain rate on both the premixed and NP flames.

The response of heptane/air partially premixed flames to the variation in strain rate is depicted in Fig. 9, which shows the shifted

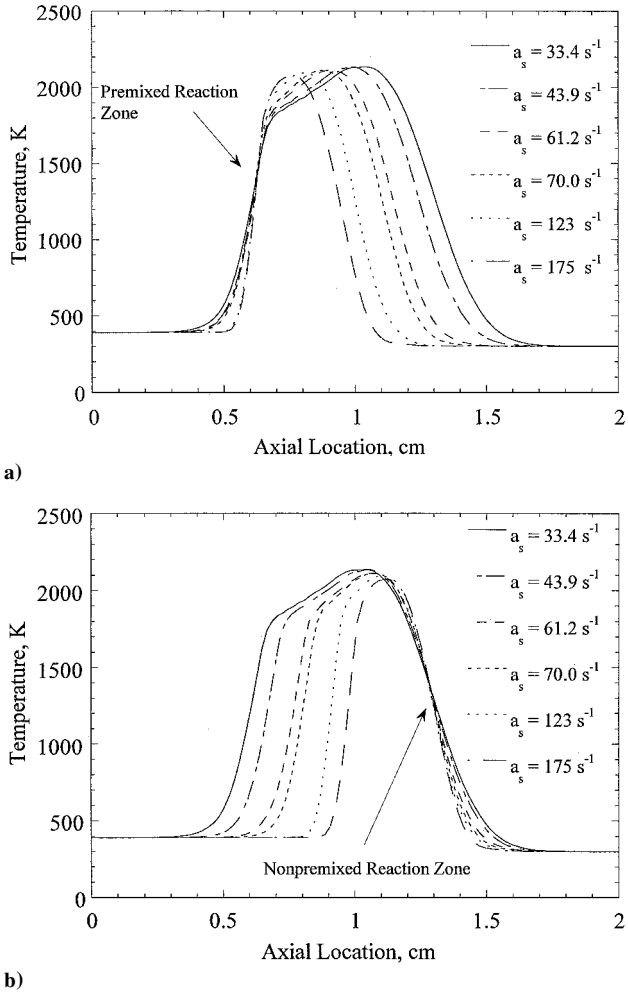

Fig. 9 Shifted temperature profiles for different strain rates obtained by collating the locations of the maximum temperature gradient in a) the premixed reaction zone and b) the NP zone; the equivalence ratio = 2.0.

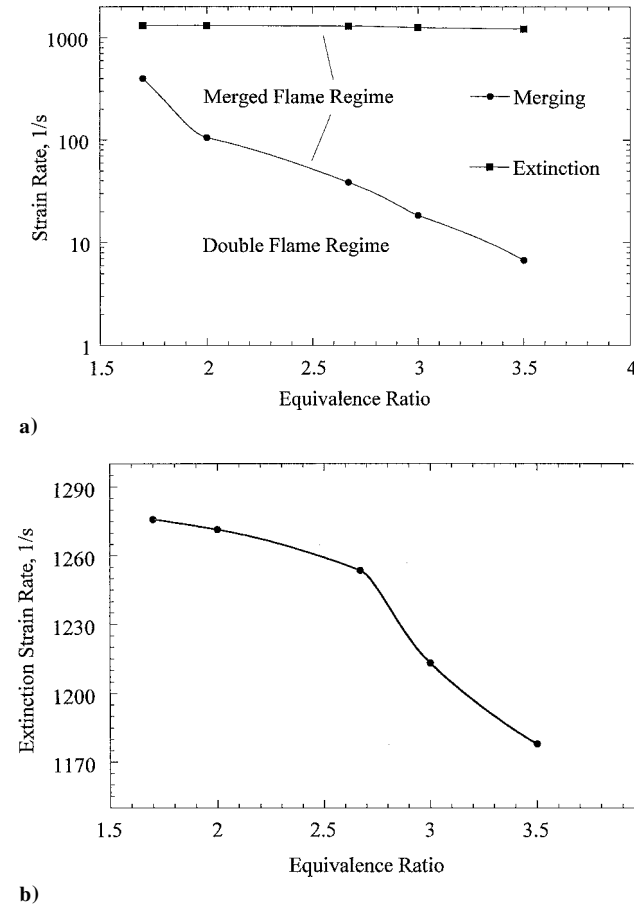

Fig. 10 Critical strain rates at reaction zones merging and flame extinction plotted vs equivalence ratio.

temperature profiles for different strain rates. The shifting is based on collating the locations of the maximum temperature gradient in the respective premixed (Fig. 9a) and NP (Fig. 9b) reaction zones. In Fig. 9a, the temperature profiles can be divided into two groups. The first group corresponding to $a_s = 34.4$, 43.9, 61.2, and 70.0 s^{-1} pertains to low and moderate strain rates and is characterized by the presence of two distinct reaction zones. The second group pertains to relatively high strain rates ($a_s = 123$ and 175 s^{-1}) for which the two reaction zones are close to merging. Within each group, the gradient of the temperature profile in the premixed zone appears to be insensitive to the strain rate. However, at $a_s = 123\ s^{-1}$, which separates the two groups, there is an abrupt change in the temperature profile gradient in the premixed zone. An analysis of the H and OH mass flux profiles (not shown) indicated that two reaction zones are distinctly separated for $a_s < 123\ s^{-1}$, whereas they start to merge at $a_s = 123\ s^{-1}$. The critical value of strain rate for merging, consequently, appears to be 123 s^{-1} for $\phi = 2.0$.

The effect of strain rate on the NP zone is similarly examined by plotting the collated temperature profiles in the NP zone, as shown in Fig. 9b. Compared to the premixed zone, the NP zone exhibits more sensitivity to the strain rate variation in that its response (characterized in terms of the temperature gradient) to the strain rate is continuous, in contrast to an abrupt change observed for the premixed zone at the merging strain rate. This suggests that the flame merging at higher strain rates affects the premixed zone more than it affects the NP zone.

Figure 10a presents the critical strain rates at reaction zones merging as a function of equivalence ratio. As indicated earlier, the merging of the reaction zones is identified by examining the mass flux profiles of H and OH radicals, from which the critical strain rate for merging can be determined. This is similar to the determination of a critical equivalence ratio for merging as discussed in the context of Fig. 8. The critical strain at flame extinction as a function of ϕ is also plotted in Fig. 10. Its variation with ϕ is more discernible in Fig. 10b. In Fig. 10a, the region below the merging curve corresponds to the double flame (partially premixed) regime, whereas the region between the two curves corresponds to the regime in which the two reaction zones are merged. As ϕ is increased (i.e., the level of partial premixing is reduced), the critical strain rate for merging decreases. At $\phi = 1.7$, the critical strain rate for merging is much higher compared to that for larger value of ϕ. In contrast, the two reaction zones begin to merge at a relatively low strain rate at $\phi \geq 3.0$.

The plot of extinction strain rate vs ϕ (cf. Fig. 10b) indicates that, as ϕ is decreased or the level of partial premixing is increased, the flame is extinguished at increasingly higher strain rates. This implies that partially premixed flames are less prone to extinction compared to NP flames, and their extinction characteristics can be improved by increasing the level of partial premixing.

State Relationships and Modified Mixture Fraction

The conserved scalar approach based on a modified mixture fraction has been effective in characterizing the flame structure and state relationships for methane/air partially premixed flames.[3,35–37] We follow a similar approach here to 1) examine the flame response to variations in ϕ and a_s and 2) characterize state relationships.

First, we employ the commonly used mixture fraction variable Z to examine the flame response to variations in ϕ. Figure 11 presents the temperature profiles with respect to Z at different ϕ. The mixture fraction Z is defined as the sum of the mass fractions of carbon and hydrogen elements originating in the fuel stream. In accord with results presented earlier, the premixed zone exhibits strong sensitivity to ϕ, whereas the NP zone is essentially insensitive to it. All temperature profiles pass through the point $T = 1760$ K, $Z = 0.108$, whereas

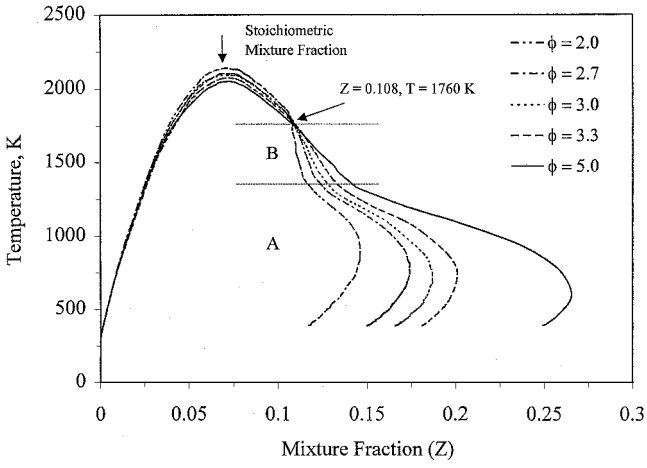

Fig. 11 Temperature vs mixture fraction for partially premixed flames established at different equivalence ratios and $a_s = 33.4\ \mathrm{s}^{-1}$.

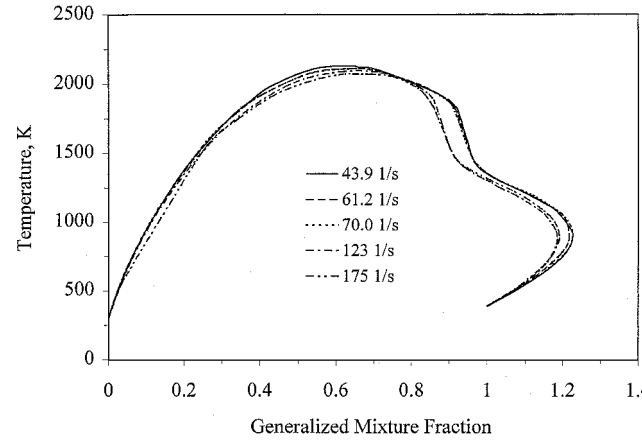

Fig. 12 State relationships in terms of temperature vs modified mixture fraction for partially premixed flames established at different strain rates and $\phi = 2.0$.

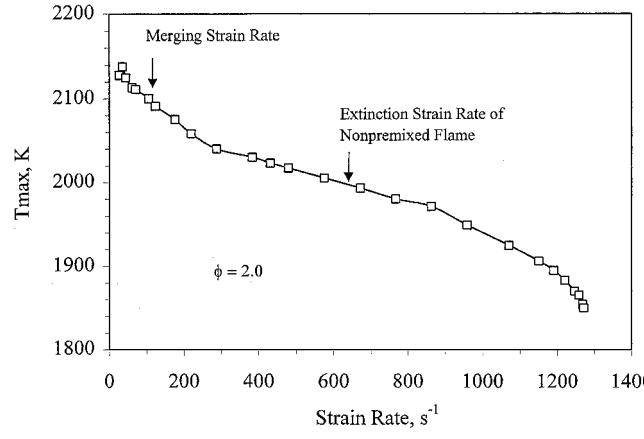

Fig. 13 Maximum flame temperature vs strain rate for partially premixed flames at $\phi = 2.0$.

they exhibit significant differences in the region $Z > 0.108$, which represents the premixed zone. The point $T = 1760$ K, $Z = 0.108$ corresponds to the peak temperature in the premixed zone. In the region $Z < 0.108$, which represents the NP zone, the temperature profiles appear to be similar, except that the peak temperature decreases as ϕ is increased. The similarity of T–Z profiles for the NP part of partially premixed flames at different ϕ can be attributed to a general characteristic of diffusion flames, for example, their structure for different ϕ is similar in the mixture fraction space. Therefore, it is reasonable to regard the point $T = 1760$ K, $Z = 0.108$ as the separation point of the two reaction zones for n-heptane/air partially premixed flames at $a_s = 33.4\ \mathrm{s}^{-1}$.

For the premixed part, the flame structure varies with respect to the fuel stream composition. In region A of Fig. 11, the mixture fraction in the fuel stream region first increases to a maximum value and then decreases continuously. This behavior is indicative of the differential diffusion effect. To characterize the effect of ϕ on the structure of premixed zone, we employ a parameter $|\mathrm{d}T/\mathrm{d}Z|$, defined as

$$\frac{\mathrm{d}T}{\mathrm{d}Z} = \frac{\mathrm{d}T/\mathrm{d}x}{\mathrm{d}Z/\mathrm{d}x}$$

In region B, $\mathrm{d}T/\mathrm{d}x$ being the temperature gradient characterizes the reaction intensity in the premixed reaction zone, whereas $\mathrm{d}Z/\mathrm{d}x$ being the concentration gradient of the fuel elements characterizes the transport intensity. A lower value of $|(\mathrm{d}T/\mathrm{d}x)/(\mathrm{d}Z/\mathrm{d}x)|$ indicates the combined effects of decreased reaction intensity and increased transport intensity. As ϕ increases, we can expect $|\mathrm{d}T/\mathrm{d}Z|$ to become smaller and approach the value corresponding to the diffusion flame as $\phi \to \infty$. The temperature profiles in region B are in accord with this observation because $|\mathrm{d}T/\mathrm{d}Z|$ decreases continuously as ϕ is increased from 2.0 to 5.0. Furthermore, as ϕ exceeds the critical value for merging ($\phi \approx 3.34$), $|\mathrm{d}T/\mathrm{d}Z|$ in region B becomes essentially identical to that of the NP zone near the point $T = 1760$ K, $Z = 0.108$; see, for example, the plot for $\phi = 5.0$.

Figure 12 presents the partially premixed flame structure with respect to the modified mixture fraction Z_m, defined as

$$Z_m = (Y - Y_{\min}/Y_{\max} - Y_{\min})$$

Here, Y denotes the sum of the local mass fractions of carbon and hydrogen elements, and $Y_{\min}$ and $Y_{\max}$ represent its values at the exit of the oxidizer and fuel nozzles, respectively. The value of Z_m exceeding unity is indicative of the differential diffusion effect. A more detailed examination indicated that this effect occurs mostly in the partially premixed combustion regime, and the value of Z_m exceeds unity in a region that is located in the upstream part of the RP zone where the fuel decomposition occurs.

The T–Z_m profiles in Fig. 12 exhibit self-similar behavior and attest that state relationships can be characterized in terms of a modified mixture fraction for heptane/air partially premixed flames. Only when the strain rate exceeds the merging strain rate ($a_s > 123\ \mathrm{s}^{-1}$), do the state relationships show some deviation. The temperature peak of the NP zone shifts lower and toward the premixed zone as a_s is increased.

From the preceding results, we infer that the strain rate variation affects the NP zone more than it affects the premixed zone. In other words, it does not affect the reactivity of the premixed fuel stream, but it does affect the balance between chemical kinetics and species transport in the NP zone. As a result, the NP zone has to shift toward the stagnation plane to counteract the enhanced transport and regain the balance. Consequently, the merging of the reaction zones at higher strain rates is a result of the NP zone shifting toward the premixed zone.

Flame Extinction

As noted in a preceding section, partially premixed flames are less prone to extinction compared to NP flames, and their extinction characteristics can be improved by increasing the level of partial premixing. The extinction state was obtained by continuously raising the strain rate by a sufficiently small step from the earlier converged solution until a "uniform temperature profile" solution (where temperature equals the boundary temperature) is obtained. The strain rate step size near the extinction state was $5.0\ \mathrm{s}^{-1}$.

Figure 13 presents the maximum flame temperature as a function of the strain rate at $\phi = 2.0$. The predicted extinction strain rate is $1271\ \mathrm{s}^{-1}$. At low strain rates, the maximum temperature $T_{\max}$ increases as a_s is increased. This is because increasing a_s causes the premixed reaction zone to move away from the boundary, which decreases heat loss to the burner. For $a_s > 33.4\ \mathrm{s}^{-1}$, the maximum temperature decreases as a_s is increased up to the extinction strain rate. As discussed in the preceding section, the two reaction zones merge at $a_s \approx 123\ \mathrm{s}^{-1}$. This implies that the flame extinction is well

preceded by the reaction zones merging. Note, however, that in the present study the radiation heat loss is not included in the analysis. As indicated by other investigations on counterflow methane/air diffusion flames,[38,39] this should affect the low-strain-rate part of the curve because the radiation heat loss constitutes a significant part of the total heat loss at low strain rates. This may lead to radiation-induced flame quenching at significantly lower strain rates. The extinction then may involve a partially premixed flame rather than an NP flame. This phenomenon has not been investigated in the present study.

Also note that the extinction strain rate of the corresponding heptane/air NP flame, computed using the same reaction mechanism and temperature boundary conditions, is 645 s^{-1}. Thus, partially premixed flames (PPFs) can sustain higher strain rates compared to the NP flames. This is due to the synergistic interactions between the two reaction zones in the case of PPFs. The computed extinction stain rate of 645 s^{-1} is also in good agreement with the measured value of 520 s^{-1} reported by Seiser et al.[25] for an NP flame with heptane/nitrogen mixture (containing 60% heptane by mass) vs air. As discussed in Ref. 25, the extinction strain rate increases as the amount of nitrogen in the heptane/nitrogen mixture is reduced.

Conclusions

The structure of n-heptane/air PPFs in a counterflow configuration has been investigated. The flame has been computed using a detailed mechanism involving 41 species and 275 elementary reactions. The simulations show excellent agreement with experimental data for laminar premixed and nonpremixed (NP) n-heptane/air flames.

For a wide range of equivalence ratios ϕ and strain rates a_s, the n-heptane/air PPF contains two spatially distinct reaction zones, namely, an RP zone on the fuel side and an NP zone on the air side. The oxidation of n-heptane under partial premixing is observed to follow two major pathways. The first one is characterized by the C_2 chemistry. The second pathway involves the formation and decomposition of C_3–C_6 olefins producing C_3H_5, which is subsequently converted to C_2 species. For the investigated conditions, interactions between the two reaction zones are characterized by the heat transport from the NP to premixed zone and the transport of CO, H_2, and C_2H_2 from the premixed to NP zone. Consequently, the chemistry of the nonpremixed reaction zone is characterized by the oxidation of CO, H_2, and C_2H_2 species.

The response of a PPF to variations in ϕ and a_s has been characterized. As ϕ or a_s is increased, the spatial separation between the two reaction zones decreases, which further enhances the thermochemical and fluid dynamic interactions between them. There is a critical value of ϕ or a_s at which the two reaction zones merge. Further increase in ϕ at a fixed a_s leads to an NP flame, whereas that in a_s at a fixed ϕ leads to flame extinction. The mass flux profiles of H and OH radicals are found to be a good indicator of reaction zones merging. The partially premixed combustion regime for n-heptane/air mixtures is obtained by computing the critical strain rate for merging as a function of the rich equivalence ratio. Results indicate that, as the level of partial premixing is reduced (i.e., ϕ is increased), the two reaction zones merge at lower strain rates.

According to temperature profiles in mixture fraction (Z) space, the variation in ϕ mostly affects the RP reaction zone, whereas that in a_s essentially affects the nonpremixed reaction zone. A parameter $|dT/dZ|$ has been used to characterize the response of the RP zone to the variation in ϕ. The insensitivity of the NP reaction zone to the variation in ϕ can be attributed to the stoichiometric-mixture characteristic of diffusion flames, which governs fuel transport in the NP zone. The sensitivity of the RP reaction zone is due to the dependence of OH concentration on the fuel mixture composition. Increasing ϕ reduces the production of OH radical, which subsequently reduces the radical pool and CO oxidation rate in the premixed zone. This results in the weakening of the RP reaction zone and its subsequent merging with the NP reaction zone.

On the other hand, the variation in a_s affects the NP reaction zone more than it affects the premixed reaction zone. Because kinetics dominates transport in the premixed zone, the fuel stream reactivity is insensitive to the strain rate. In contrast, transport effects are more important in the NP reaction zone, which renders it more sensitive to the strain rate variation. A modified mixture fraction has been found to be effective in characterizing the PPF structure and its response to variation in ϕ and a_s.

Stretch-induced extinction of n-heptane/air PPFs has been investigated. Results indicate that as the level of partial premixing is increased, the flame extinction occurs at increasingly higher strain rates, implying that PPFs are less prone to extinction compared to NP flames. In addition, it is observed that in the partially premixed combustion regime, the critical strain rate for reaction zones merging is significantly smaller than that for flame extinction. This implies that the flame extinction is well preceded by the merging of the reaction zones.

Acknowledgments

This research was supported by the National Science Foundation Combustion and Plasma Systems Program through Grant CTS-9707000, for which Farley Fisher is the Program Director. We fully acknowledge the contribution of F. L. Dryer for providing the n-heptane oxidation mechanism. Many fruitful discussions with I. K. Puri are gratefully appreciated.

References

[1] Shu, Z., Krass, B. J., Choi, C. W., Aggarwal, S. K., Katta, V. R., and Puri, I. K., "Experimental and Numerical Investigation of the Structure of Steady Two-Dimensional Partially Premixed Methane–Air Flames," *Proceedings of the Combustion Institute*, Vol. 27, Combustion Inst., Pittsburgh, PA, 1998, pp. 625–632.

[2] Blevins, L., and Gore, J. P., "Computed Structure of Low Strain Rate Partially Premixed Flames," *Combustion and Flame*, Vol. 116, No. 4, 1999, pp. 546–566.

[3] Shu, Z., Choi, C. W., Aggarwal, S. K., Katta, V. R., and Puri, I. K., "Gravity Effects on Steady Two-Dimensional Partially Premixed Methane–Air Flames," *Combustion and Flame*, Vol. 118, No. 1, 1999, pp. 91–107.

[4] Li, S. C., and Williams, F. A., "NOx Formation in Two-Stage Methane–Air Flames," *Combustion and Flame*, Vol. 118, No. 3, 1999, pp. 399–414.

[5] Li, S. C., and Williams, F. A., "Counterflow Heptane Flame Structure," *Proceedings of the Combustion Institute*, Vol. 28, Combustion Inst., Pittsburgh, PA, 2000, pp. 1031, 1038.

[6] Haworth, D. C., Blint, R. J., Cuenot, B., and Poinsot, T. J., "Numerical Simulation of Turbulent Propane–Air Combustion with Nonhomogeneous Reactants," *Combustion and Flame*, Vol. 121, No. 3, 2000, pp. 395–417.

[7] Flynn, F. F., Durrett, R. P., Hunter, G. L., Loye, A. O., Akinyemi, O. C., Dec, J. E., and Westbrook, C. K., "Diesel Combustion: An Integrated View Combining Laser Diagnostics, Chemical Kinetics, and Empirical Validation," Society of Automotive Engineers, SAE Paper 99-01-0509, 1999.

[8] Aggarwal, S. K., "Review of Spray Ignition Phenomena: Present Status and Future Research," *Progress in Energy and Combustion Science*, Vol. 24, No. 6, 1998, pp. 565–600.

[9] Aggarwal, S. K., "Dominant Ignition Modes in Liquid Fuel Sprays: A Review of Droplet Ignition Phenomena," American Society of Mechanical Engineers Petroleum Div., 1998.

[10] Warnatz, J., "Chemistry of High Temperature Combustion of Alkanes up to Octane," *Proceedings of the Combustion Institute*, Vol. 20, Combustion Inst., Pittsburgh, PA, 1984, pp. 845–856.

[11] Chevalier, C., Pitz, W. J., Warnatz, J., Westbrook, C. K., and Melenk, H., "Hydrocarbon Ignition: Automatic Generation of Reaction Mechanisms and Applications to Modeling of Engine Knock," *Proceedings of the Combustion Institute*, Vol. 24, Combustion Inst., Pittsburgh, PA, 1992, pp. 93–101.

[12] Davis, S. G., and Law, C. K., "Laminar Flame Speeds and Oxidation Kinetics of iso-Octane–Air and n-Heptane–Air Flames," *Proceedings of the Combustion Institute*, Vol. 27, Combustion Inst., Pittsburgh, PA, 1998, pp. 521–527.

[13] Card, J. M., and Williams, F. A., "Asymptotic Analysis with Reduced Chemistry for the Burning of n-Heptane Droplets," *Combustion and Flame*, Vol. 91, No. 1, 1992, pp. 187–199.

[14] Marchese, A. J., Dryer, F. L., and Nayagam, V., "Numerical Modeling of Isolated n-Alkane Droplet Flames: Initial Comparisons with Ground and Space-Based Microgravity Experiments," *Combustion and Flame*, Vol. 116, No. 3, 1999, pp. 432–459.

[15] Choi, M.Y., Mulholland, G.W., Hamins, A., and Kashiwagi, T., "Comparisons of the Soot Volume Fraction Using Gravimetric and Light Extinction Techniques," *Combustion and Flame*, Vol. 102, No. 1, 1995, pp. 161–169.

[16] Gutheil, E., and Sirignano, W. A., "Counterflow Spray Combustion Modeling with Detailed Transport and Detailed Chemistry," *Combustion and Flame*, Vol. 113, No. 1, 1998, pp. 92–105.

[17] Dec, J. E., "A Conceptual Model of DI Diesel Combustion Based on Laser-Sheet Imaging," Society of Automotive Engineers, SAE Paper 970873, 1997.

[18]Held, T. J., Marchese, A. J., and Dryer, F. L., "A Semi-Empirical Reaction Mechanism for n-Heptane Oxidation and Pyrolysis," *Combustion Science and Technology*, Vol. 123, 1997, pp. 107–146.

[19]Müller, U. C., Peters, N., and Linan, A., "Global Kinetics for n-Heptane Ignition at High Pressures," *Proceedings of the Combustion Institute,* Vol. 24, Combustion Inst., Pittsburgh, PA, 1992, pp. 777–784.

[20]Bakali, A. E., Delfau, J., and Vovelle, C., "Modeling of a Rich, Atmospheric Pressure, Premixed n-Heptane/O_2/N_2 Flame," *Combustion and Flame*, Vol. 118, No. 3, 1999, pp. 381–398.

[21]Bollig, M., Pitsch, H., Hewson, J. C., and Seshadri, K., "Reduced n-Heptane Mechanism for Non-Premixed Combustion with Emphasis on Pollutant-Relevant Intermediate Species," *Proceedings of the Combustion Institute,* Vol. 26, Combustion Inst., Pittsburgh, PA, 1996, pp. 729–737.

[22]Li, S. C., Libby, P. A., Williams, F. A., "Experimental and Theoretical Studies of Counterflow Spray Diffusion Flames," *Proceedings of the Combustion Institute,* Vol. 24, Combustion Inst., Pittsburgh, PA, 1992, pp. 1503–1512.

[23]Chen, N. H., Rogg, B., Bray, N. C., "Modelling Laminar Two-Phase Counterflow Flames with Detailed Chemistry and Transport," *Proceedings of the Combustion Institute*, Vol. 24, Combustion Inst., Pittsburgh, PA, 1992, pp. 1513–1521.

[24]Chelliah, H. K., Bui-Pham, M., Seshadri, K., and Law, C. K., "Numerical Description of the Structure of Counterflow Heptane–Air Flames Using Detailed and Reduced Chemistry with Comparison to Experiments," *Proceedings of the Combustion Institute,* Vol. 24, Combustion Inst., Pittsburgh, PA, 1992, pp. 851–857.

[25]Seiser, R., Truett, L., Trees, D., and Seshadri, K., "Structure and Extinction of Non-Premixed n-Heptane Flames," *Proceedings of the Combustion Institute*, Vol. 27, Combustion Inst., Pittsburgh, PA, 1998, pp. 649–657.

[26]Lutz, A. E., Kee, R. J., Grcar, J. F., and Rupley, F. M., "OPPDIF: A Fortran Program for Computing Opposed-Flow Diffusion Flames," Sandia National Labs., Rept. SAND96-8243, 1996.

[27]Kee, R. J., Rupley, F. M., Miller, J. A., "Chemkin: A Fortran Chemical Kinetics Package for the Analysis of Gas Phase Chemical Kinetics," Sandia National Labs., Rept. 89-8009B, 1994.

[28]Chelliah, H. K., Law, C. K., Ueda, T., Smooke, M. D., and Williams, F. A., "An Experimental and Theoretical Investigation of the Dilution, Pressure and Flow-Field Effects on the Extinction Condition of Methane–Air–Nitrogen Diffusion Flames," *Proceedings of the Combustion Institute*, Vol. 23, Combustion Inst., Pittsburgh, PA, 1990, pp. 503–511.

[29]Tanoff, M. A., Smooke, M. D., Osborne, R. J., Brown, T. M., and Pitz, R. W., "The Sensitive Structure of Partially Premixed Methane–Air vs. Air Counterflow Flames," *Proceedings of the Combustion Institute*, Vol. 26, Combustion Inst., Pittsburgh, PA, 1996, pp. 1121–1128.

[30]Giovangigli, V., and Smooke, M. D., "Extinction of Strained Premixed Laminar Flames with Complex Chemistry," *Combustion Science and Technology*, Vol. 53, 1987, pp. 23–49.

[31]Gacar, J. F., Kee, R. J., Smooke, M. D., and Miller J. A., "A Hybrid Newton/Time-Integration Procedure for the Solution of Steady, Laminar, One-Dimensional, Premixed Flames," *Proceedings of the Combustion Institute*, Vol. 21, Combustion Inst., Pittsburgh, PA, 1986, pp. 1773–1782.

[32]Xue, H. S., and Aggarwal, S. K., "The Structure of Two-Stage Counterfow n-Heptane–Air Flames," American Society of Mechanical Engineers, ASME Paper 2000-GT-134, May 2000.

[33]Shu, Z., Katta, V. R., Puri, I. K., and Aggarwal, S. K., "Effects of C_2-Chemistry on the Structure of Partially Premixed Methane–Air Flames," *Combustion Science and Technology*, Vol. 157, 2000, pp. 185–211.

[34]Law, C. K., Sung, C. J., Yu, G., and Axelbaum, R. L., "On the Structural Sensitivity of Purely Strained Planar Premixed Flames to Strain Rate Variations," *Combustion and Flame*, Vol. 98, No. 1, 1994, pp. 139–154.

[35]Aggarwal, S. K., and Puri, I. K., "Flame Structure Interactions and State Relationships in an Unsteady Partially Premixed Flame," *AIAA Journal*, Vol. 36, No. 7, 1998, pp. 1190–1199.

[36]Krass, B. J., Zellmar, B. W., Puri, I. K., and Singh, S., "Applications of Flamelet Profiles to Flame Structure in Practical Burners," *Journal of Energy Resources Technology*, Vol. 121, No. 1, 1999, pp. 66–72.

[37]Williams, F. A., "Progress in Knowledge of Flamelet Structure and Extinction," *Progress in Energy and Combustion Science*, Vol. 26, Nos. 4–6, 2000, pp. 657–682.

[38]Ju, Y. G., Guo, H. S., Maruta, K., and Liu, F. S., "On the Extinction and Flammability Limit of Non-Adiabatic Stretched Methane–Air Flames," *Journal of Fluid Mechanics*, Vol. 342, 1997, pp. 315–334.

[39]Chao, B. H., and Law, C. K., "Asymptotic Theory of Flame Extinction with Surface Radiation," *Combustion and Flame*, Vol. 92, No. 1, 1993, pp. 1–24.

J. P. Gore
Associate Editor